IJIE

Journal homepage: http://penerbit.uthm.edu.my/ojs/index.php/ijie
ISSN : 2229-838X e-ISSN : 2600-7916

The International Journal of Integrated Engineering

Stress Intensity Factors for Circumferential Semi-Elliptical Cracks in Cylinders Subjected to Forced Convection Heat Transfer

S. M. Nabavi [1*], M. B. Shahmorady [2]

Faculty of Aerospace Engineering, Malek Ashtar University of Technology, Tehran, IRAN

* Corresponding Author

DOI: https://doi.org/10.30880/ijie.2020.12.04.021
Received 1 January 2020; Accepted 13 May 2020; Available online 15 May 2020

Abstract: This paper analyzes the circumferential semi-elliptical crack on the inner surface of a thick-walled cylinder while keeping the thermal loading in steady state. Forced convection heat transfer in the inner surface and free convection in the outer surface are applied to the cylinder, which was constructed from isotropic and homogeneous materials. To this end, the thermal stress intensity factors are determined using the weight function method. To validate the results, 3-D finite element method is applied as well as API standard code. Due to the existence of two planes of symmetry, only a quarter model of the cylinder was used and along the crack front, the modelling is carried out over singular isoparametric elements. The results for stress intensity factor are obtained at different aspect ratios and relative depths of the crack. The stress intensity factors calculated via built-in J-integral solver based on the domain integral technique in the ABAQUS software. The results obtained via this method were in good agreement with the proposed weight function, demonstrating the latter's high adequacy and efficiency.

Keywords: Weight function, circumferential semi-elliptical crack, finite element analysis, thermal stress intensity factor, cylinder

Nomenclature

a	crack depth
a/t	relative depth
B_i, B_o	Biot numbers
E	Young's modulus
h_i, h_o	convection coefficients
k	thermal conductivity
K	stress intensity factor (SIF)
K_T	thermal SIF
$m(r,a)$	weight function
R_i	inner radius of cylinder
R_o	outer radius of cylinder
u	radial displacement
α	thermal conductivity
Γ	Gamma function
μ	shear modulus of the material

* *Corresponding author: nabavi@mut.ac.ir*

ν Poisson's ratio
θ temperature
θ_i, θ_o surrounding fluid temperatures
σ_Z axial stress

1. Introduction

One important consideration in structural health monitoring is assessing the growth rate of a detected crack to determine the limits of the admissible flaw in the component. For this purpose, determination of stress intensity factors with high efficacy and accuracy is necessary. Various approaches have been proposed to calculate the stress intensity factor (SIF), including the finite element (FE) method [1-3], the weight function (WF) method [4,5], the semi-analytical approach [6], and empirical methods [7], as well as using influence factors in standard codes such as API 579 [8], BS 7910 [9], ASME Section XI [10] and R6 [11]. Al-Moayed et al. [12] employed FE software ANSYS to determine the SIFs for a single semi-elliptical circumferential crack on a pressurized thick cylinder. Carpinteri et al. [13-17] analysed the influence of notches on the SIFs for a circumferential part-through flaw. The crack is assumed to exist at the notch root (reduced cross-section) in the cases of pipes, round bars, and double-curvature shells. The SIF values along the crack front are determined through a three-dimensional FE analysis. Ismail et al. [18, 19] investigated a round bar containing a circumferential semi-elliptical crack under combined loading using ANSYS FE software. The SIF values were obtained along the crack front employing the J-integral procedure.

Each method has its own merits. For crack modelling, the numerical methods are time-consuming, particularly in dealing with 3D surface cracks wherever fine meshes around the 3D crack front are essential. WF method requires deriving the crack weight function. The experimental method is expensive because it involves accurate test equipment. In standard codes, the analysis of highly gradient actual loadings such as thermal stress distribution often gets complicated. Depending on the loading and the issue at hand, one might take any of the above approaches.

In a recent effort, Zareei and Nabavi [4] derived the WF of circumferential semi-elliptical cracks in the inner surface of the cylinder (Fig. 1) which can be applied to any arbitrary loading. The steady-state thermal SIFs obtained using the WF and compared with those achieved through 3D FE modelling and API 579 standard code. The three-dimensional analysis is performed on a cylinder with an internal circumferential semi-elliptical crack of depth a and length 2c. For each crack geometry, i.e. for any given aspect ratio (a/c) and relative depth (a/t), the SIFs may be calculated via built-in J-integral solver based on the domain integral technique in the ABAQUS software [20]. In order to demonstrate the reliability of each FE model of the cracked cylinder, J values have been checked to be independent of the path, a large enough number of convergence tests have been tested and obtained SIFs were independent of the number of elements.

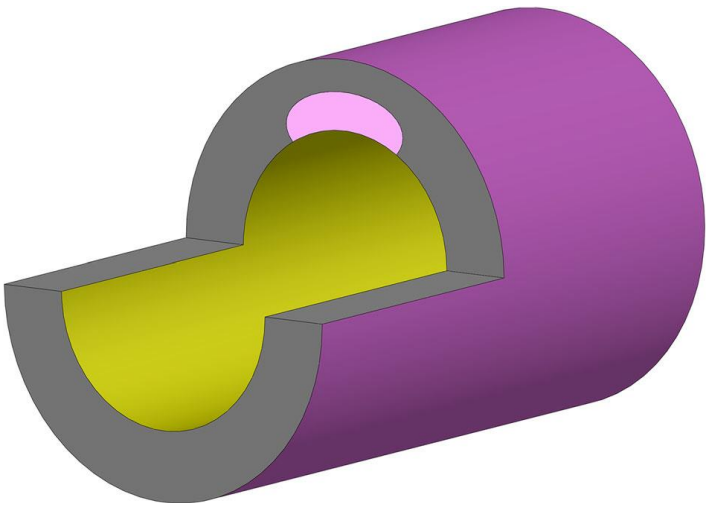

Fig. 1 - Schematic view of an internal circumferential semi-elliptical crack in a pipe

2. Determination of Steady State Thermal Stresses

A long hollow cylinder was constructed from an isotropic and homogeneous material, and its inner and outer radii of the cylinder are represented with R_i and R_o, respectively. The equations of axisymmetric thermoelasticity in cylindrical coordinates are as follows [21]

$$\frac{\partial^2 \theta}{\partial r^2} + \frac{1}{r}\frac{\partial \theta}{\partial r} = 0 \tag{1}$$

$$\frac{\partial^2 u}{\partial r^2}+\frac{1}{r}\frac{\partial u}{\partial r}-\frac{u}{r^2}-\frac{\alpha(1+\nu)}{1-\nu}\frac{\partial \theta}{\partial r}=0 \tag{2}$$

where θ and u are the steady-state temperature and displacement distributions, respectively, and α and ν are the material properties such as the thermal expansion coefficient and the Poisson's ratio, respectively. The inner and outer surfaces of the cylinder are subjected to convective heat transfer with the convection coefficients h_i and h_o, respectively and are traction free. The environment temperatures of the inner and outer fluid are θ_i and θ_o, respectively. As a result, the thermal boundary conditions are:

$$k\frac{\partial \theta}{\partial r}=h_i(\theta-\theta_i) \qquad \text{on} \qquad r=R_i \tag{3a}$$

$$-k\frac{\partial \theta}{\partial r}=h_o(\theta-\theta_o) \qquad \text{on} \qquad r=R_o \tag{3b}$$

Using steady-state heat transfer equation (eq. 1), the temperature distribution was obtained:

$$\theta(r)=\zeta_1+\zeta_2\,Log(r/R_o)+\zeta_3\,Log(r/R_i) \tag{4}$$

in which

$$\zeta_2=-\theta_i/\psi \tag{5a}$$

$$\zeta_3=-\theta_o/\psi \tag{5b}$$

$$\zeta_1=\zeta_3/B_i-\zeta_2/B_o \tag{5c}$$

$$\psi=1/B_i+1/B_o+Log(R_o/R_i) \tag{5d}$$

where $B_i=R_ih_i/k$ and $B_o=R_oh_o/k$ are the Biot numbers and k is the thermal conductivity of cylinder. The radial displacement distribution will be extracted by applying the thermal solution (eq. 4) into eq. 2 as

$$u(r)=\frac{r\beta}{2}\zeta_1+\frac{r\beta}{4}\zeta_2\left(2Log(r/R_o)-1\right)+\frac{r\beta}{4}\zeta_3\left(2Log(r/R_i)-1\right)+C_1r+C_2/r \tag{6}$$

where $\beta=\alpha(1+\nu)/(1-\nu)$, and the unknowns parameters C_1 and C_2 may be determined by applying the mechanical boundary conditions. Both the inner and outer surfaces of the cylinder are traction free. This means that the radial stresses are negligible on both sides of the cylinder. After some simplification which are not given for the sake of brevity, the longitudinal stress distribution can be computed as

$$\sigma_Z(r)=-2\mu\beta\left(\zeta_1+\zeta_2Log(\frac{r}{R_o})+\zeta_3\,Log(\frac{r}{R_i})\right)+\frac{4\mu\nu}{(1-2\nu)}C_1 \tag{7}$$

in which

$$C_1=\frac{\alpha(2\nu^2+\nu-1)}{4(\nu-1)(R_i^2-R_o^2)}\left(R_i^2\left(2\zeta_1+(2Log(\frac{R_i}{R_o})-1)\zeta_2-\zeta_3\right)+R_o^2\left(-2\zeta_1+\zeta_2+\zeta_3+2Log(\frac{R_i}{R_o})\zeta_3\right)\right) \tag{8}$$

where μ denotes the shear modulus. When the temperature of the inner fluid is less than the outer one, tensile stress achieves at the inner surface of the cylinder and cause the opening mode to occur.

3. The WF Method to Determine SIFs

Weight function of a cracked body is dependent on the shape of the crack and independent of the loading. Determination of this function is essential to obtain SIFs under any stress distribution if the symmetry and mode of loading do not change. Zareei and Nabavi [4] developed the four-term WF for the deepest point of a circumferential semi-elliptical crack in a cylinder as follows:

$$m(r,a)=\sqrt{\frac{2}{\pi}}\sqrt{\frac{1}{R_i+a-r}}+3\sqrt{\frac{2}{\pi}}\frac{1}{a}\sqrt{R_i+a-r}+M_1\sqrt{\frac{2}{\pi a}}+M_2\sqrt{\frac{2}{\pi a^3}}(R_i+a-r) \tag{9}$$

in which the crack tip placed in $r=R_i+a$, and M_1 and M_2 represented in terms of relative depth and aspect ratio values using two reference loads [4]. Using this WF, the SIFs for any arbitrary loading can be calculated as:

$$K=\int_{R_i}^{R_i+a}\sigma(r)m(r,a)dr \tag{10}$$

where $\sigma(r)$ is the ɹongitudinal stress distribution in an uncracked cylinder. The accuracy of the weight function depends on reference loading. For the purpose of analysis of the uncracked cylinder, an nth-order curve was fitted to the thermal stress distribution as:

$$\sigma_{thermal} = \sum_{j=0}^{n} A_j \, x^j \tag{11}$$

where x represents a vector from the inner toward the outer surface of the cylinder, and the A_i coefficients are achieved from the curve fitting. The SIFs are obtained using the thermal stress distribution and the WF integral (eq. 10) as follow

$$K_{thermal}(a) = \sqrt{\frac{2a}{\pi}} \sum_{j=0}^{n} A_j \, a^n \left(\frac{\sqrt{\pi}\,\Gamma(j+1)}{\Gamma(j+\frac{1}{2})} + \frac{3\sqrt{\pi}\,\Gamma(j+1)}{2\Gamma(j+\frac{5}{2})} + \frac{1}{j+1} M_1 + \frac{1}{j^2+3j+2} M_2 \right) \tag{12}$$

where Γ is the Gamma function. Hence, the first step in this process is to determine the steady-state thermal stress distribution of the uncracked cylinder. The coefficients in Eq. 11 are then computed using the polynomial curve fitted to the stress distribution. Finally, the thermal SIFs are derived using Eq. 12 conveniently.

4. 3D FE Modeling to Determine SIFs

3D FE has been employed to model cracked cylinder using ABAQUS software. Due to the existence of two planes of symmetry, only a quarter model of the cylinder was used. Along the crack front, the modelling was performed over singular isoperimetric elements by displacing the mid-node to quarter-node, and in other segments, 20-node elements were used (Fig. 2). In order to investigate thermal SIFs, at first, the heat transfer problem was solved in ABAQUS and then used the results to estimate the uncoupled thermal stress. Finally, using a path independent J-integral in the software, the values of thermal SIFs were calculated as:

$$K_T = \sqrt{EJ/(1-v^2)} \tag{13}$$

where E denotes the Young's modulus. In each stage, the convergence and accuracy of results were tested to ensure the validity of modelling.

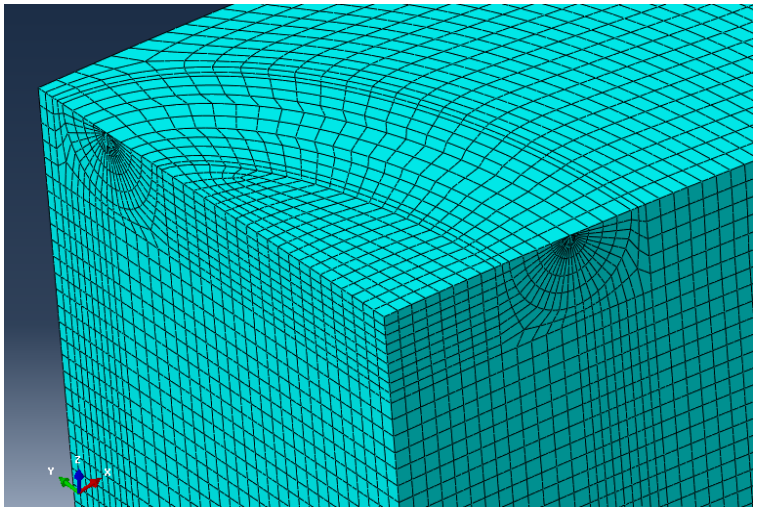

Fig. 2 - 3D FE modeling of circumferential semi-elliptical crack

5. Standard Codes in Determination of SIFs

Solution method in ASME [10], R6 [11] and API [8] is based on the influence factors. The first two standards employ a cubic polynomial curve fitted to the stress distribution across the position of crack face, whereas the API standard employs a 4th-order curve fitted to the stress distribution across wall thickness of the cylinder. Subsequently, all three models use the available influence factors in standards to obtain the SIFs. BS7910 [9] takes the more conservative approach of using the linear approximation of the longitudinal stress distribution. On the other hand, the API standard is simpler than other codes because it carries out the fitting only once. Moreover, its stress distribution estimation is more accurate due to the higher order of fitting.

6. Results and Validation

To verify the efficiency of the derived WF, dimensionless values of steady-state thermal SIFs $K_N = K_T(1-v)/\left(E\alpha(\theta_o-\theta_i)\sqrt{\pi(R_o-R_i)}\right)$ for different crack's geometries were analyzed and compared with the other two methods. Crack dimensions in a limited relative depth (0.1-0.8) with an aspect ratio of 0.2 to 1 are applicable. The SIFs were evaluated for values of $E=207GPa$, $v=0.3$, $\alpha=12e-6$ 1/°C, and the ratio of the outer-to-inner radius of the cylinder was $R_o/R_i=1.10$. The thermo-mechanical material properties were assumed constant for thermal analysis purposes. The cylinder was subjected to forced convection heat transfer in the inner surface and free convection in its outer one. The temperature of the inner fluid was kept at $\theta_i=-100\,°C$. The outer surface of the cylinder retained in a permanent thermal condition with surrounding temperature $\theta_o=0\,°C$ and free convection with $B_o=100$. The results of four aspect ratios of 0.25, 0.5, 0.75 and 1 are depicted in Figs 3 to 6 for different values of Biot numbers (B_i) in the inner surface of the cylinder.

As it can be seen, the higher the Biot number, the higher the thermal SIFs, meaning that as more heat penetrates inside the wall due to increased forced convection heat transfer, it more significantly contributes to increase SIFs. The good agreement of the results of the three methods with each other is also indicated. One interesting finding is that the more extended the crack (the lower aspect ratio), the more critical the deep cracks will be. On the other hand, the more circular the crack is, the maximum values of SIFs tend to be reminiscent of shallow cracks. It means that in certain geometric dimensions, shallow cracks happen to be more critical than deeper ones. Another important finding is that in any state of loading, values of SIFs decrease with increasing the aspect ratio in all relative depths. The rate of reduction in deep cracks is higher than shallow cracks.

According to the above data, since the weight function is independent of the loading, it can be used in cases of more complicated loadings and higher gradients and therefore has a considerable advantage over other methods.

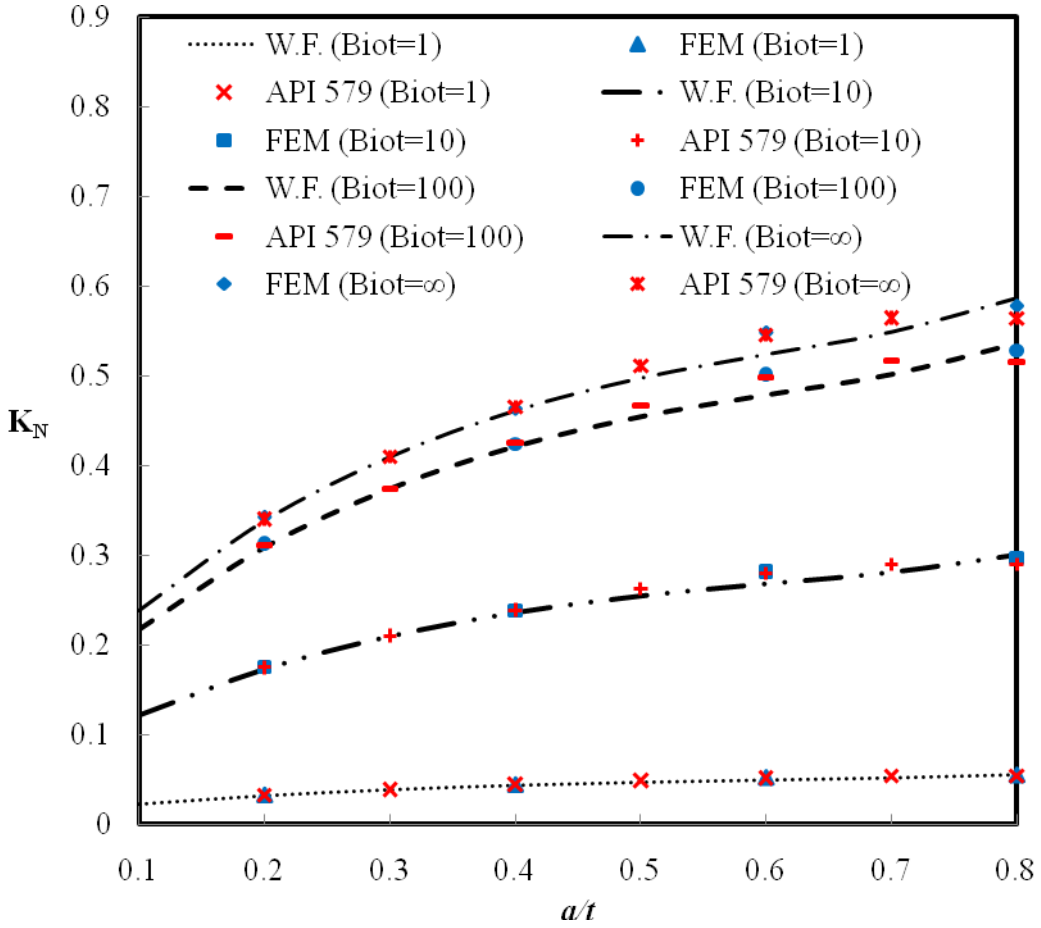

Fig. 3 - Comparison of dimensionless thermal SIF in terms of forced convection in the inner surface of cylinder with aspect ratio of 0.25

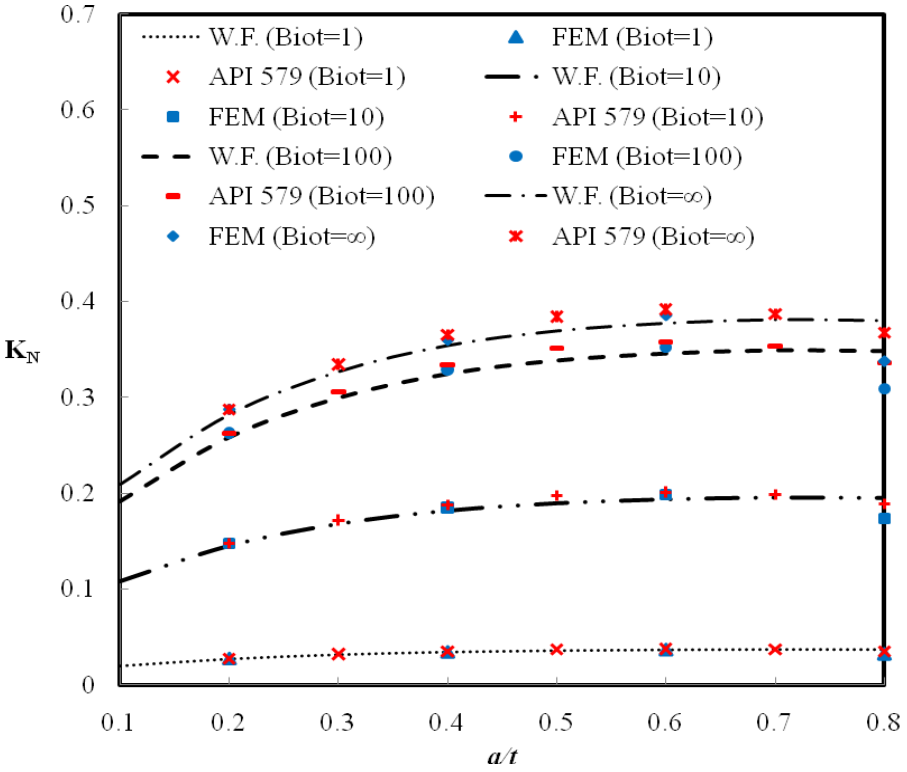

Fig. 4 - Comparison of dimensionless thermal SIF in terms of forced convection in the inner surface of cylinder with aspect ratio 0.5

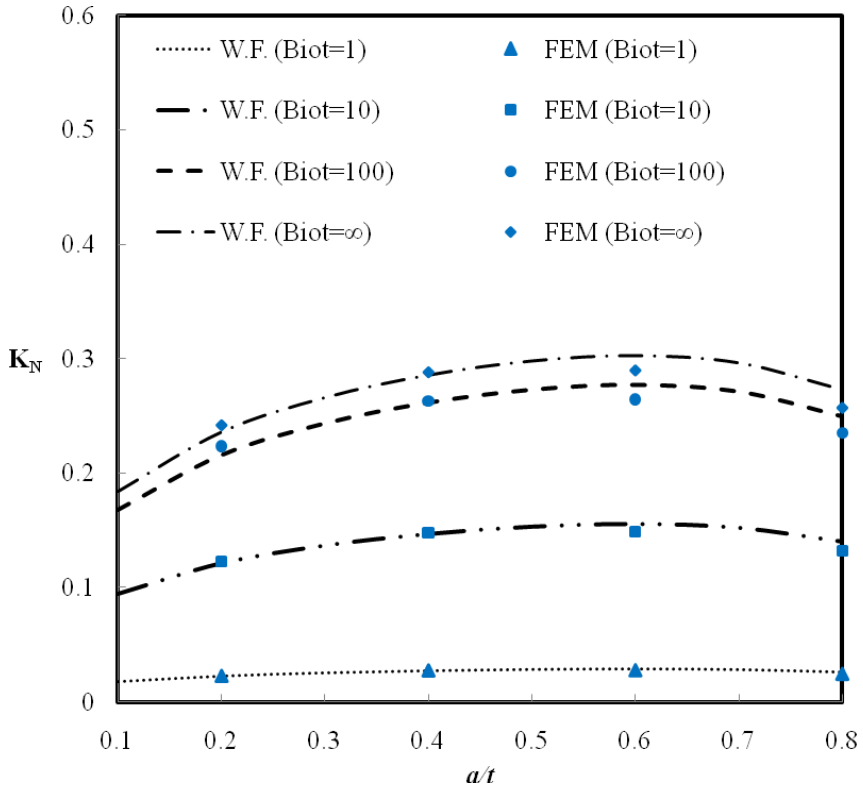

Fig. 5 - Comparison of dimensionless thermal SIF in terms of forced convection in the inner surface of cylinder with aspect ratio of 0.75

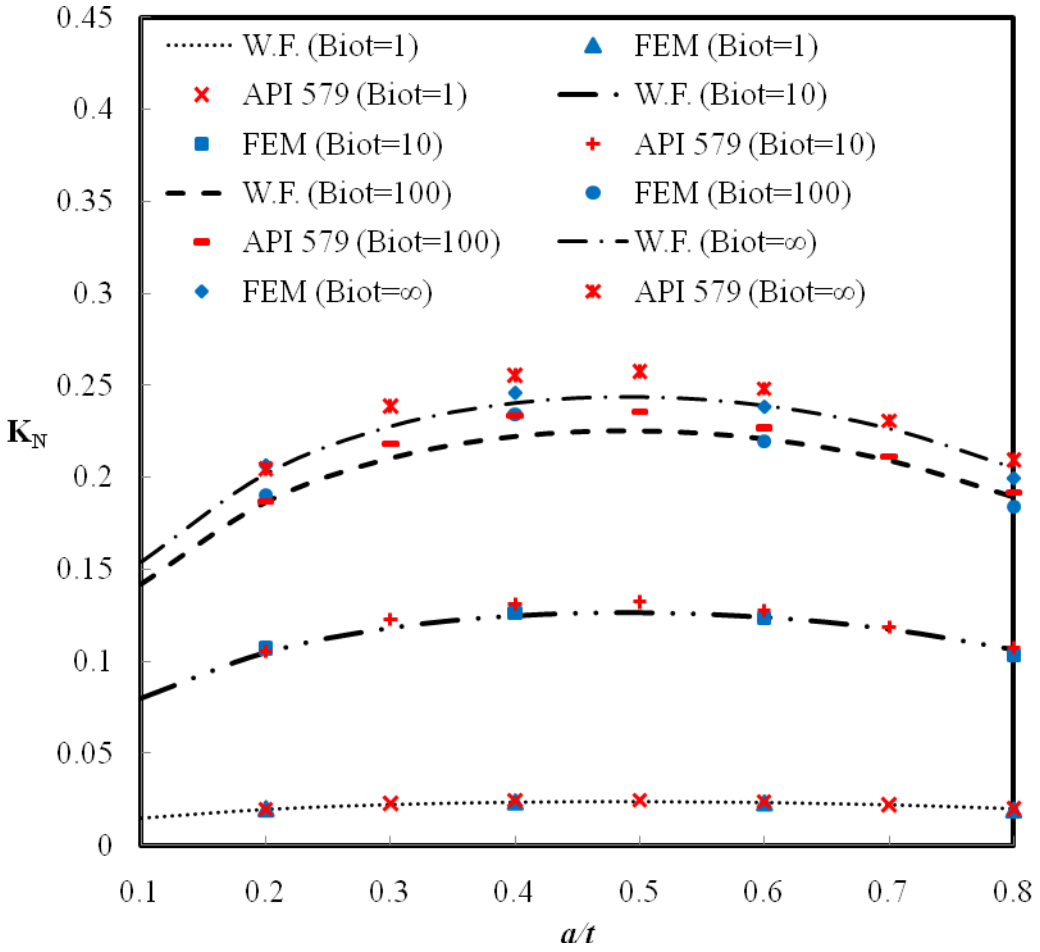

Fig. 6 - Comparison of dimensionless thermal SIF in terms of forced convection in the inner surface of cylinder with aspect ratio 1

7. Conclusion

In the present work, the SIFs under steady-state thermal loading are estimated using the WF method and FE analysis and 3D modelling of the circumferential semi-elliptical crack in the cylinder. Various range of crack geometries correspond to different relative depths and aspect ratios was considered to calculate thermal SIFs. The results depicted for different values of Biot numbers in the inner surface of the cylinder four aspect ratios of 0.25, 0.5, 0.75 and 1. The efficiency and accuracy of the derived WF was examined by 3D FE analysis and API standard code. Comparison of the findings with those of 3D FE analysis and API code confirms a good agreement.

References

[1] Poette, C., Albaladejo, S. (1991). Stress intensity factors and influence functions for circumferential surface cracks in pipes. Engineering Fracture Mechanics, 39, 641–650.
[2] Bergman M. (1995). Stress intensity factors for circumferential surface cracks in pipes. Fatigue and Fracture of Engineering Materials and Structures, 18, 1155-72.
[3] El Hakimi A, Le Grognec P, Hariri S. (2008). Numerical and analytical study of severity of cracks in cylindrical and spherical shells. Engineering Fracture Mechanics, 75, 1027-1044.
[4] Zareei A., Nabavi S.M. (2016). Weight function for circumferential semi-elliptical cracks in cylinders due to residual stress fields induced by welding. Archive of Applied Mechanics, 86, 1219-1230.
[5] Zareei A., Nabavi S.M. (2016). Calculation of stress intensity factors for circumferential semielliptical cracks with high aspect ratio in pipes. International Journal of Pressure Vessels and Piping, 146, 32-38.
[6] Wallbrink, C.D., Peng, D., Jones, R. (2005). Assessment of partly circumferential cracks in pipes. International Journal of Fracture, 133, 167–181.
[7] Xian-Ming K., Si-Tao Z., Zhen-Yuan C. (1989). Studies on stress intensity factor of surface cracks in a cylinder under remote tension loads. Engineering Fracture Mechanics, 33, 105-11.
[8] API 579 Fitness-for-Service, (2007). (2nd ed.). American Petroleum Institute: Washington DC.

[9] BS 7910 Guide on Methods for Assessing the Acceptability of Flaws in Metallic Structures, British Standards Institution, London, UK (2013).
[10] ASME. ASME boiler and pressure vessel code, Sec. IX, (2007).
[11] R6, Revision 4: Assessment of the integrity of structures containing defects (2013). Gloucester, UK: EDF Energy Nuclear Generation Ltd.
[12] Al-Moayed O.M., Kareem A.K., Ismail A.E., Jamian S., Nemah M.N. (2019) Distribution of mode I stress intensity factors for single circumferential semi-elliptical crack in thick cylinder. International Journal of Integrated Engineering, 11(7), 102-111.
[13] Carpinteri A., Brighenti R., Vantadori S. (2003). Circumferentially notched pipe with an external surface crack under complex loading. International Journal of Mechanical Sciences, 45 (12), 1929-1947.
[14] Carpinteri A., Vantadori S. (2009). Sickle-shaped cracks in metallic round bars under cyclic eccentric axial loading. International Journal of Fatigue, 31 (4), 759-765.
[15] Carpinteri A., Ronchei C., Vantadori S. (2013). Stress intensity factors and fatigue growth of surface cracks in notched shells and round bars: two decades of research work. Fatigue and Fracture of Engineering Materials and Structures, 36 (11), 1164-1177.
[16] Carpinteri A., Brighenti R., Vantadori S. (2006). Notched shells with surface cracks under complex loading. International Journal of Mechanical Sciences, 48 (6), 638-649.
[17] Carpinteri A., Brighenti R., Vantadori S. (2009). Notched double-curvature shells with cracks under pulsating internal pressure. International Journal of Pressure Vessels and Piping, 86 (7), 443-453.
[18] Ismail A.E., Ariffin A.K., Abdullah S. Ghazali M.J. (2012). Stress intensity factors for surface cracks in round bar under single and combined loadings. Meccanica, 47, 1141-1156.
[19] Ismail A.E., Ariffin A.K., Abdullah S., Ghazali, M.J. (2017). Finite element analysis of J-integral for surface cracks in round bars under combined mode I loading. International Journal of Integrated Engineering, 9(2), 1-8.
[20] ABAQUS, (2014) User's manual, version 6.14, Dassault Systèmes Inc., USA.
[21] Hetnarski R.B., Eslami M.R. (2019). Thermal Stresses - Advanced Theory and Applications. 2nd Edition, Springer.